Front. Optoelectron. 2014, 7(1): 53–58
DOI 10.1007/s12200-013-0380-4

RESEARCH ARTICLE

Misalignments among stacked layers of metamaterial terahertz absorbers

Yinghui GUO[1], Lianshan YAN (✉)[1], Wei PAN[1], Bin LUO[1], Xiantao ZHANG[1], Xiangang LUO[2]

1 Center for Information Photonics & Communications, School of Information Science & Technology, Southwest Jiaotong University, Chengdu 610031, China
2 State Key Lab of Optical Technology for Microfabrication, Institute of Optics and Electronics, Chinese Academy of Sciences, Chengdu 610029, China

Abstract Misalignment among stacked layers of absorbers is inevitable in practice. Adverse effects induced by this undesired factor was investigated and analyzed in this paper. The absorption responses of thin terahertz metamaterial (MM) absorber with different degree of misalignment were simulated by finite-difference time-domain (FDTD) method under both transverse magnetic (TM) and transverse electric (TE) polarization. Results show that slight misalignment deteriorates absorption response due to the decreased spatial resolution. The analyses are given in terms of the magnetic field distribution in the cross section. In addition, the depravation is changed with polarization, which depends on the direction of excursion.

Keywords metamaterials (MMs), terahertz absorber, misalignment, subwavelength structure

1 Introduction

Metamaterials (MMs) are artificial materials consisting of periodically patterned subwavelength unit cell to gain properties that may not be found in nature. Due to its exotic electromagnetic properties, MMs are applied in many potential fields, such as perfect lenses [1], electromagnetic cloaks [2], negative refractive index materials [3], electromagnetically induced transparency like transmission [4] and thin absorbers [5]. By adjusting the effective ε (permittivity) and μ (permeablility) of the MMs, absorption close to unity is possible. MMs absorbers in terahertz regime are especially important due to scarcity in this frequency and beyond the thickness limitations of traditional devices. So far, many efforts have been taken to design and fabricate the omnidirectional, polarization-insensitive, and broadband MMs absorbers [6–11]. Cui et al. proposed an ultra broadband thin-film infrared absorber made of saw-toothed anisotropic MM [6] and an omnidirectional, polarization-insensitive and broadband thin absorber in the terahertz regime [7]. Ma et al. reported a dual band [8] and a broadband [9] polarization insensitive MM absorber in terahertz. Utilizing trapezoid gratings arrays, Aydin et al. designed a broadband polarization-independent super absorber [10]. By engineering the frequency dispersion, a broadband infrared absorption was realized [11].

In these schemas, alternately stacked metal-insulator-metal (MIM) layers are widely used due to their excellent electromagnetic responses. However, because of the limit accuracy of the manufacturing process, misalignment among the stacked layers of absorbers is inevitable in practice. Unfortunately, this practical factor is not taken into account in previous studies and perfect alignment among them is taken for granted. Although Chen et al. have discussed the misalignment effects in MMs absorbers [12], it is still worthy to investigate this effect on absorbers with different structures due to its structural-dependent characteristics.

2 Model and simulations

First, we investigated a simplified single-channel terahertz absorber deposited on a glass substrate, which is consisting of a metallic ring patterned on a metallic film with a polymer layer in between. Three-dimensional oblique view and two-dimensional side view are shown in Figs. 1(a) and 1(b), respectively, with period $P = 26\,\mu m$ in x and y directions. To investigate the absorption properties of the proposed structure, numerical simulations were performed by finite-difference time-domain (FDTD) method (Lume-

Received September 22, 2013; accepted November 1, 2013

E-mail: lsyan@home.swjtu.edu.com, guoyinghui8@163.com

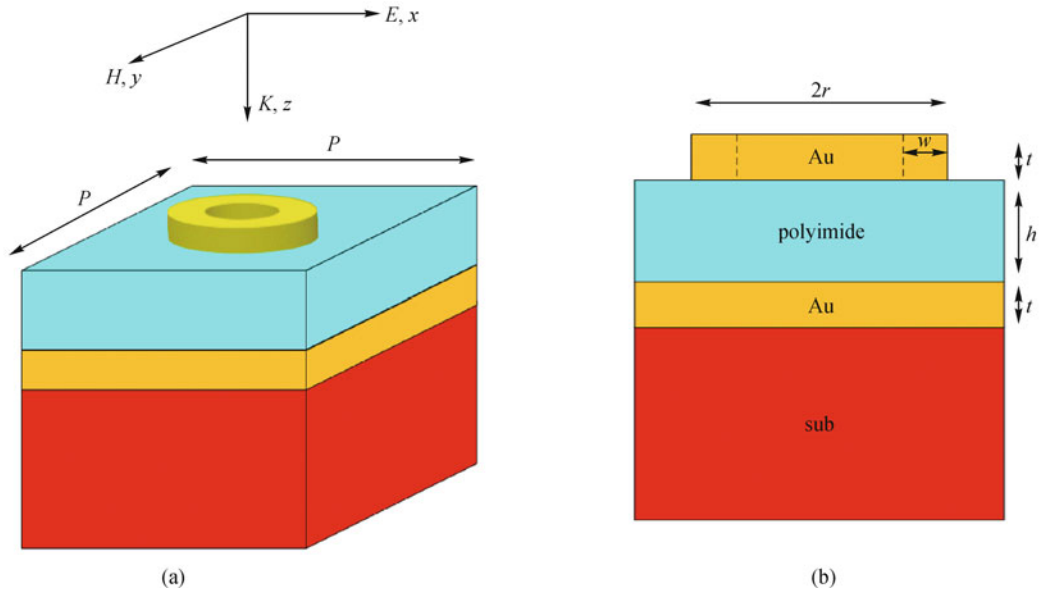

Fig. 1 Schematic unit cell of terahertz absorbers. (a) Three-dimensional oblique view; and (b) two-dimensional side view

rical Solution, Inc.). The grid sizes in x, y and z direction were chosen to be 0.2, 0.2 and 0.5 μm to ensure convergence. Due to the structural symmetry, the proposed absorber is insensitive to the incidence polarization. The lossy polymer with index $n = 1.8 + 0.06i$ [9] was used in our simulation and the thickness of gold (Au) t was set as 0.2 μm through the paper. Due to the gold (Au) layer performs as a perfect electrical conductor (PEC) in the terahertz and the thickness of the metallic ground plane is much larger than the typical skin depth, the transmission from the structure is totally suppressed. Consequently, the absorption can be calculated directly through the reflectivity by $A = 1 - R$. To obtain a perfect absorber, we set $r = 6$ μm, $w = 1$ μm and adjust the thickness of polymer layer h to realize impedance matching with free space (i.e., $Z = \sqrt{\varepsilon/\mu} = 1$), minimizing the reflectance to zero. The reflection spectra with different h are shown in Fig. 2(a), which show the reflectivity at the resonant dip changes with the separation distance, consisting with previous literature [7]. Specially, when $h = 2.7$ μm the reflection is greatly suppressed ($< 0.1\%$) at resonant frequency $f = 5.49$ THz. Therefore, a perfect terahertz absorber at 5.49 THz is realized with $\lambda/18$ structural thickness. In addition, the evolution of resonant wavelength with the radius r is also plotted and shown in Fig. 2(b), which shows the resonance wavelengths are proportional to the radius r without significant change of the reflectance intensity. Thus, the absorption frequency can be adjusted by the radius while the absorption is almost invariable.

Subsequently, we investigated a broadband terahertz

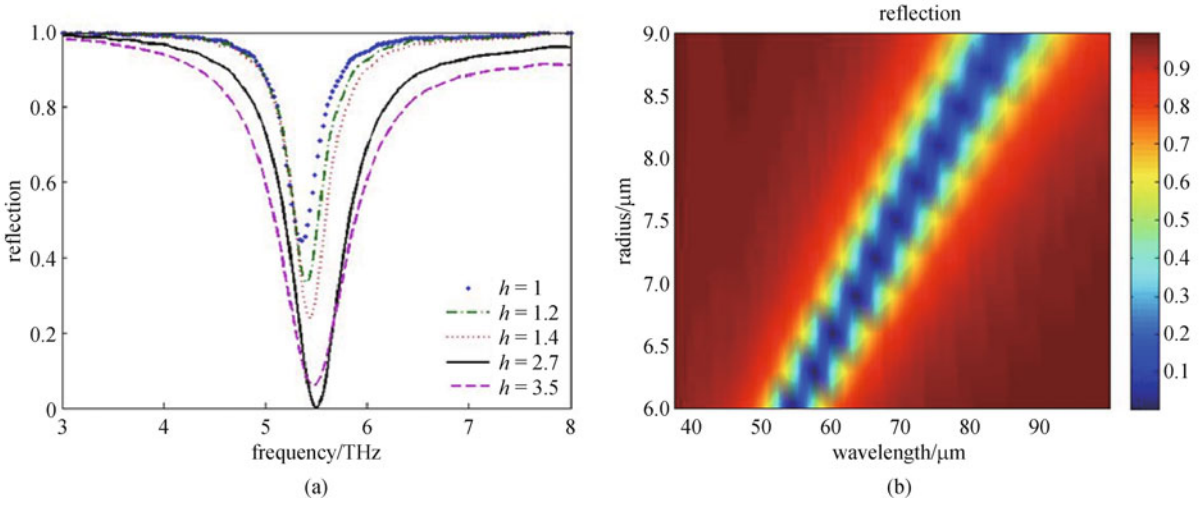

Fig. 2 (a) Reflection spectra for different polymer thickness h; (b) resonance wavelengths evolution with the radius of ring r

absorber by alternatively stacking three metallic rings with different radius in the polymer layer, as shown in Figs. 3(a) and 3(b). The simulated absorption responses are shown in Fig. 3(c), with corresponding parameter values listed in Table 1. We can see three absorption peaks appears at frequencies of 4.394, 3.757, and 3.192 THz with absorptivity of 0.955, 0.985, 0.950, respectively. Moreover, a wide absorption frequency-band from 3.0 to 4.7 THz was obtained with the absorption greater than 0.6. Note that, the frequency range of the broadband absorber can be changed by adjusting the radius of the metallic rings. Meanwhile, the thickness of the proposed absorber was still quite thin.

To understand the origin of the absorption response, the profile of the magnetic field at $y = 0$ plane for the three absorption-peaks (i.e., 3.192, 3.757, and 4.394 THz) are plotted and shown in Fig. 4. It can be found that strong magnetic field is confined among the three layers, indicating all the three rings contribute to each resonant absorption-peak (i.e., a hybrid mode). However, it is worth to be noted that the magnetic field profiles of absorption peaks at $y = 0$ plane own different distributions. As the dot lines box shown in Figs. 4(a)–4(c), the magnetic field profiles in the x-z plane depend on the dimension extensions of the rings I, II and III in x and z direction, respectively.

3 Misalignment effects and discussion

To investigate the misalignment effects among the metallic rings and determine how this factor affects the absorption, lateral shifts in x direction Sx were introduced among them,

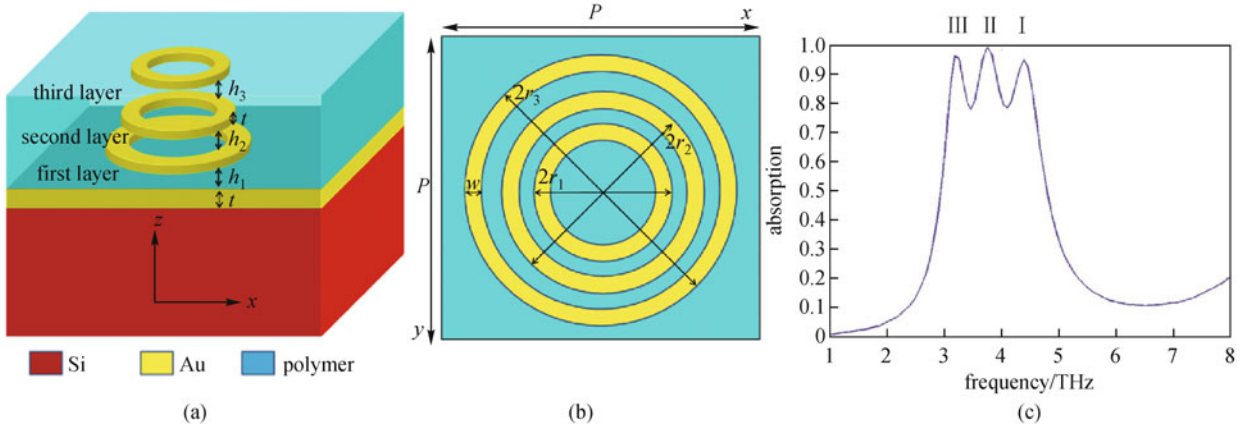

Fig. 3 Schematic unit cell of broadband terahertz absorbers. (a) Three-dimensional oblique view; (b) top view with defined parameters; and (c) corresponding absorption spectra

Table 1 Geometric parameters of the broadband terahertz absorber

parameters	P	r_1	r_2	r_3	h_1	h_2	h_3	w	t
value/μm	22	6.7	7	8	4.5	0.2	0.3	1	0.2

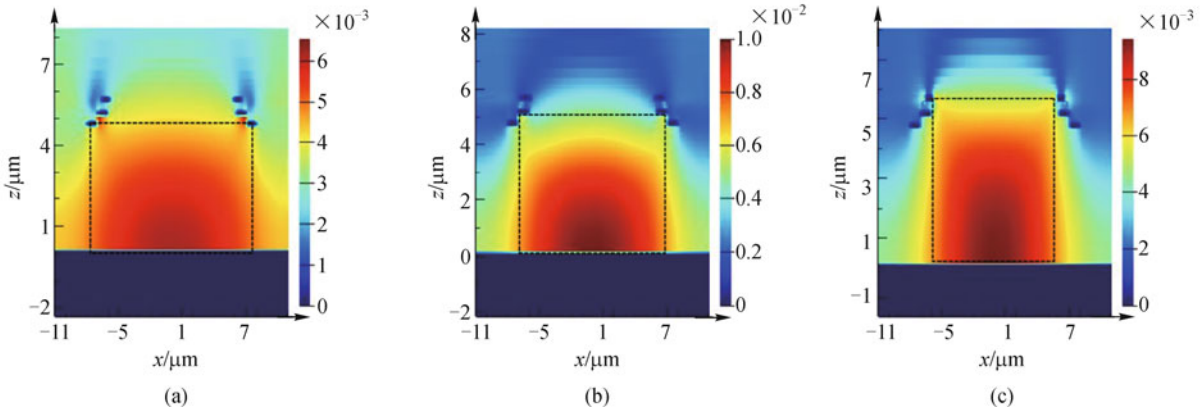

Fig. 4 Magnetic field profile at $y = 0$ planes for three absorption peaks of absorber. (a) III; (b) II; and (c) I. Dotted line: main area of field distributions

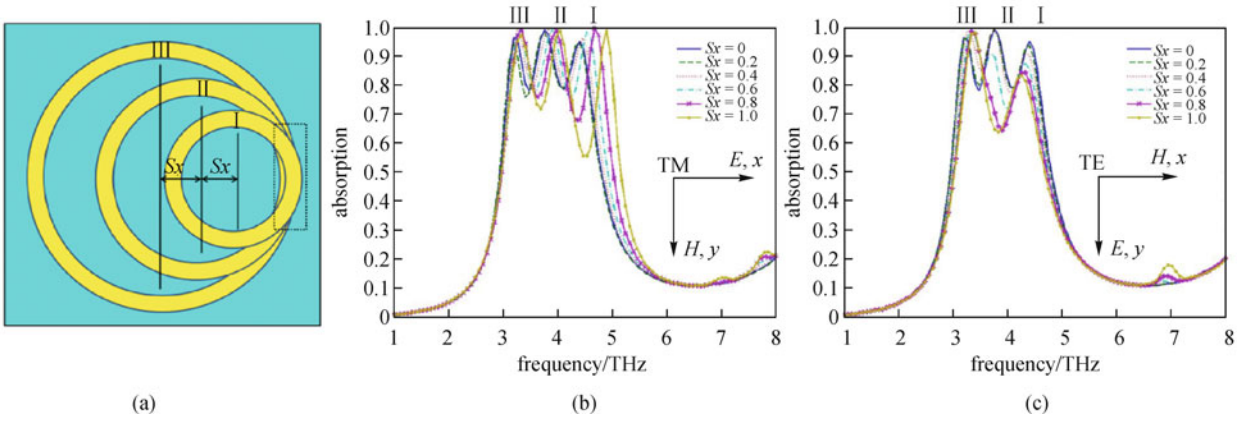

Fig. 5 Top view of the structure with a lateral shift *Sx* in the *x* direction (a); absorption responses with *Sx* from 0 to 1 μm under transverse magnetic (TM) (b) and transverse electric (TE) polarization (c)

as shown in Fig. 5(a). The introduction of the misalignment in *x* direction breaks the symmetric of the structure in *x*-*y* plane, which results in different absorption response to the TM and TE polarization incidence. The simulated absorption responses are shown in Figs. 5(b) and 5(c), respectively. It can be seen that, for the TM polarization incidence, absorption peaks exhibit different levels of blue shifts with *Sx* increased from 0 to 1 μm. Note that, the shift of peak I is faster than that of peaks II and III, which cause the absorptivity between the peaks I and II decrease. Specially, the absorptivity drops below 0.6 at 4.5 THz with misalignment degree *Sx* = 1.0 μm. To find the underlying reasons for the blue shifts, magnetic field profiles and the charge density distributions of the absorption peaks at $y = 0$ plane are plotted and shown in Figs. 6 and 7, respectively. One can see that, when *Sx* = 1.0 μm the extension of ring II in + *x* direction is superimposed with ring I, which cause the ring II cannot be distinguished, as illustrated in the dot line box in Fig. 5(a). Therefore, the space discrimination resolution decreases and the charge density of ring II after misalignment (Fig. 7(a)) is greatly reduced compared with the cases without misalignment (Fig. 7(b)). In this case, the magnetic field profile of peak I and peak II in *x* direction not only depends on the lateral extension of corresponding ring, but also is limited by other two rings, which cause the charge density increases in the high discrimination resolution areas (Figs. 7(a) and 7(f)). In this case, the extension of magnetic resonance in *x* direction decreases, as the dot line box shows in Figs. 6(c) and 6(b), which is the main reason for the blue shift of peak I and peak II. On the contrary, the profile extension in *x* direction is nearly invariable for rings III at this time, as indicated by Fig. 6(a). Thus, inconspicuous blue shift is observed for peaks III.

For the TE polarization incidence, both absorption peak II and peak I shift to low frequency while peak III shifts to high frequency with the increasing misalignment degree resulting the merging of peak II and peak III at $Sx > 0.8$ μm. In order to explain the different behaviors among three peaks, electric profiles of three rings at peak III are simulated and plotted. As presented in Fig. 8, electrical resonances are excited in all the three rings indicating a

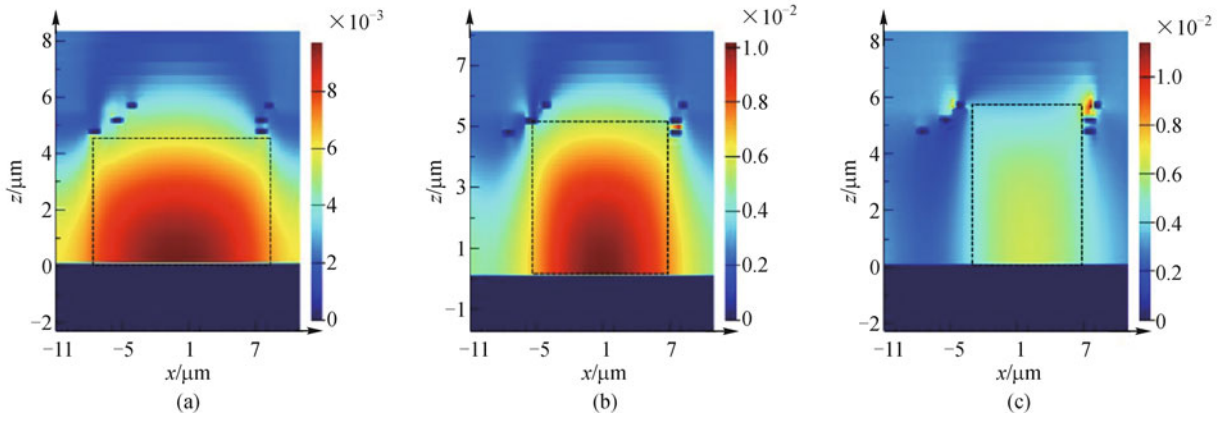

Fig. 6 Magnetic field profile $|H_y|^2$ at $y = 0$ plane with TM polarization incidence for peaks (a) III; (b) II and (c) I when *Sx* = 1.0 μm. Dotted line: main area of field distributions

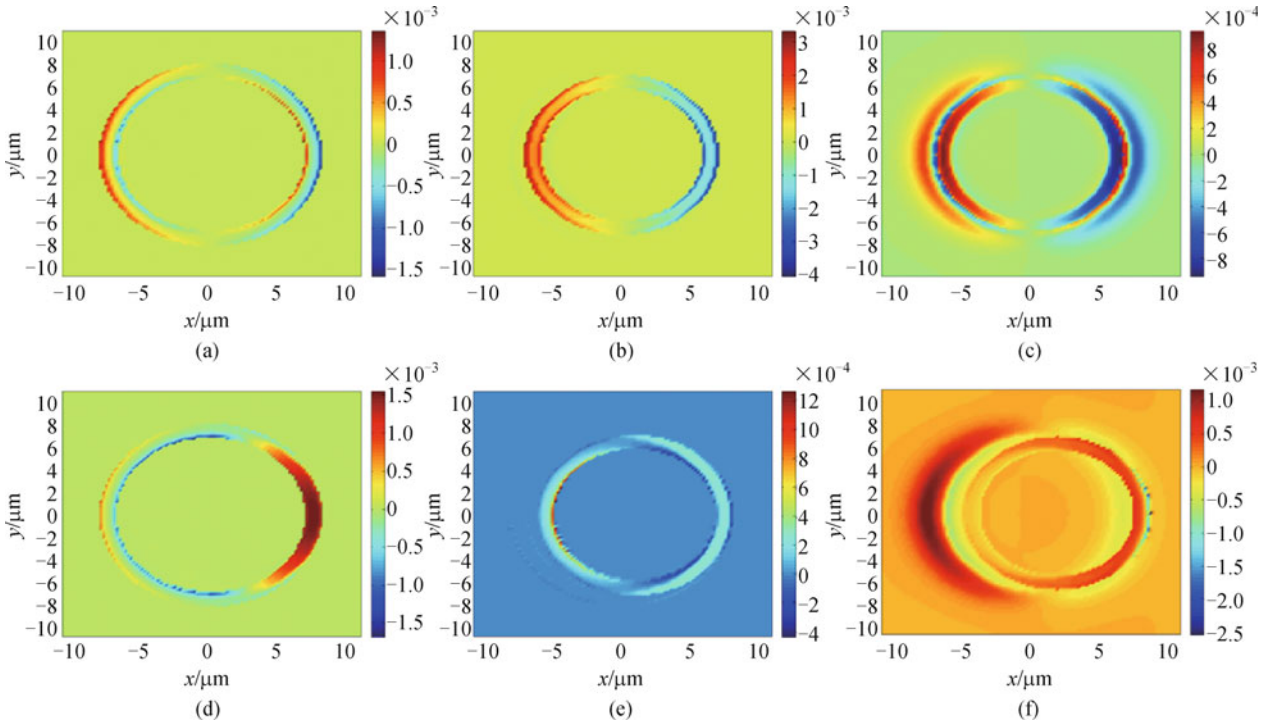

Fig. 7 Charge density distribution at three metallic rings for TM polarization. (a)–(c) Three metallic rings without misalignment; (d)–(f) three metallic rings with Sx = 1.0 μm. (a) and (d) III; (b) and (e) II; (c) and (f) I

hybrid mode among them at peak III and ring III exhibits the strongest resonance. In specific, ring III coupling with other two rings resulting in a decreasing dimension extension in electric field profile at x-y plane (Fig. 8(a)), while ring II and ring I coupling with ring III resulting in an increasing dimension extension in electric field profile at x-y plane (Figs. 8(b) and 8(c)). Therefore, peak III shifts to a high frequency, meanwhile peak II and peak I shift to low frequencies. Consequently, the absorption peaks II and III merge together with increasing misalignment Sx. Note that, a small absorption peak at 6.95 THz for TE polarization appears due to the misalignment, as show in Fig. 5(c). In order to find the behind reason, simulations with same misalignment Sx = 1.0 μm but different periods 20, 25 and 30 μm were carried out. The simulated results are shown in Fig. 9, from which one can find the small absorption peak gradually decreases with increasing period. Thus, the small absorption may be due to the coupling between neighboring unit cells resulting from the misalignment (i.e., ring I in one unit coupling with ring III in the neighboring unit).

4 Conclusions

In conclusion, misalignments among the stacked layers of the thin absorbers were investigated by FDTD method. Simulation results shows that even a slight misalignment have serious influence on the absorption response, which was analyzed in terms of the magnetic field profiles. It was found that the misalignments decreased the space resolu-

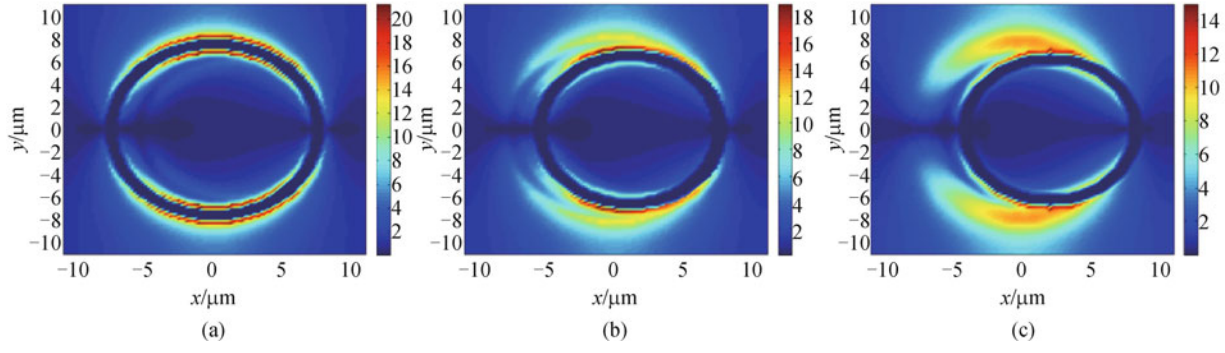

Fig. 8 Electric field profile of three rings at peak III at x-y plane for TE polarization with Sx = 1.0 μm. (a) Ring III; (b) ring II; and (c) ring I

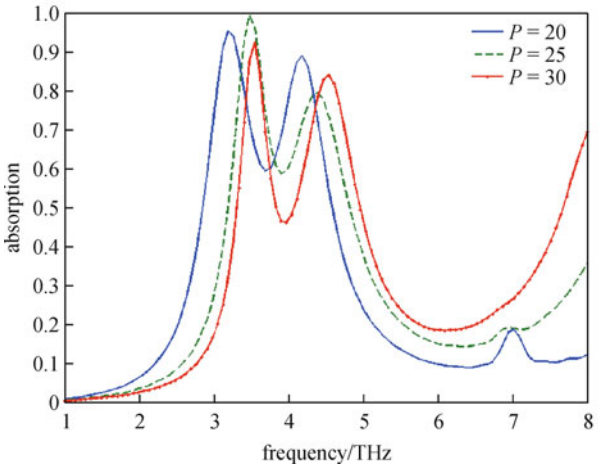

Fig. 9 Absorption spectra for TE polarization with different period when Sx = 1.0 μm

tion, which is the main reason for deteriorated absorption response. Therefore, a well-designed structure with high space resolution is significant to overcome the influences of misalignments, which may provide a guide for the design of broadband MMs absorbers.

Acknowledgements This work was supported by the National Basic Research Program of China (Nos. 2013CBA01700 and 2012CB315704), the National Natural Science Foundation of China (Grant No. 61325023), and the Funds for the Excellent Ph.D. Dissertation of Southwest Jiaotong University in 2012.

References

1. Pendry J B. Negative refraction makes a perfect lens. Physical Review Letters, 2000, 85(18): 3966–3969
2. Valentine J, Li J S, Zentgraf T, Bartal G, Zhang X. An optical cloak made of dielectrics. Nature Materials, 2009, 8(7): 568–571
3. Shelby R A, Smith D R, Schultz S. Experimental verification of a negative index of refraction. Science, 2001, 292(5514): 77–79
4. Guo Y H, Yan L S, Pan W, Luo B, Wen K H, Guo Z, Luo X G. Electromagnetically induced transparency (EIT)-like transmission in side-coupled complementary split-ring resonators. Optics Express, 2012, 20(22): 24348–24355
5. Landy N I, Bingham C M, Tyler T, Jokerst N, Smith D R, Padilla W J. Design, theory, and measurement of a polarization-insensitive absorber for terahertz imaging. Physical Review B: Condensed Matter and Materials Physics, 2009, 79(12): 125104–125109
6. Cui Y X, Fung K H, Xu J, Ma H J, Jin Y, He S L, Fang N X. Ultrabroadband light absorption by a sawtooth anisotropic metamaterial slab. Nano Letters, 2012, 12(3): 1443–1447
7. Ye Y Q, Jin Y, He S L. Omnidirectional, polarization-insensitive and broadband thin absorber in the terahertz regime. JOSA B, 2010, 27(3): 498–504
8. Ma Y, Chen Q, Grant J, Saha S C, Khalid A, Cumming D R S. A terahertz polarization insensitive dual band metamaterial absorber. Optics Letters, 2011, 36(6): 945–947
9. Grant J, Ma Y, Saha S, Khalid A, Cumming D R S. Polarization insensitive, broadband terahertz metamaterial absorber. Optics Letters, 2011, 36(17): 3476–3478
10. Aydin K, Ferry V E, Briggs R M, Atwater H A. Broadband polarization-independent resonant light absorption using ultrathin plasmonic super absorbers. Nature Communication, 2011, 2: 517
11. Feng Q, Pu M B, Hu C G, Luo X G. Engineering the dispersion of metamaterial surface for broadband infrared absorption. Optics Letters, 2012, 37(11): 2133–2135
12. Chen Q, Sun F H, Song S C. Subcell misalignment in vertically cascaded metamaterial absorbers. Optics Express, 2013, 21(13): 15896–15903